*R*esearch in
*A*stronomy and
*A*strophysics

Influence of a scalar-isovector δ-meson field on the quark phase structure in neutron stars

Grigor Bakhshi Alaverdyan

Yerevan State University, Yerevan 0025, Armenia; *galaverdyan@ysu.am*

Abstract The deconfinement phase transition from hadronic matter to quark matter in the interior of compact stars is investigated. The hadronic phase is described in the framework of relativistic mean-field theory, where the scalar-isovector δ-meson effective field is also taken into account. The MIT bag model for describing a quark phase is used. The changes of the parameters of phase transition caused by the presence of a δ-meson field are explored. Finally, alterations in the integral and structural parameters of hybrid stars due to both a deconfinement phase transition and inclusion of a δ-meson field are discussed.

Key words: dense matter — equation of state — mean-field — stars: neutron — quark

1 INTRODUCTION

The structure of compact stars functionally depends on the equation of state (EOS) of matter in a sufficiently wide range of densities, from $7.9\,\mathrm{g\,cm^{-3}}$ (the endpoint of thermonuclear burning) to one order of magnitude higher than nuclear saturation density. Therefore, the study of properties and composition of the constituents of matter in the extremely high density region is of great interest in both nuclear and neutron star physics. The relativistic mean-field (RMF) theory (Walecka 1974; Serot & Walecka 1986, 1997) has been effectively applied to describe the structure of finite nuclei (Lalazissis et al. 1997; Typel & Wolter 1997), the features of heavy-ion collisions (Ko & Li 1996; Prassa et al. 2007), and the equation of state (EOS) of nuclear matter (Müller & Serot 1995). Inclusion of the scalar-isovector δ-meson in this theoretical scheme and investigation of its influence on low density asymmetric nuclear matter was performed in Refs. Kubis & Kutschera (1999); Liu et al. (2002); Greco et al. (2003). At sufficiently high density, different exotic degrees of freedom, such as pion and kaon condensates, in addition to deconfined quarks, may appear in the strongly interacting matter. The modern concept of a hadron-quark phase transition is based on the feature of that transition, that is the presence of two conserved quantities in this transition: baryon number and electric charge (Glendenning 1992). It is known that, depending on the value of surface tension σ_{s}, the phase transition of nuclear matter into quark matter can occur in two scenarios (Heiselberg et al. 1993; Heiselberg & Hjorth-Jensen 2000): ordinary first order phase transition with a density jump (Maxwell construction), or formation of mixed hadron-quark matter with a continuous variation of pressure and density (Glendenning construction) (Glendenning 1992). Uncertainty of the surface tension values does not allow us to determine the phase transition scenario, which actually takes place. In our recent paper (Alaverdyan 2009a), under the assumption that the transition to quark

matter is a usual first-order phase transition, which can be described by the Maxwell construction, we have shown that the presence of the δ-meson field leads to the decrease of transition pressure P_0 and coexistence of baryon number densities n_N and n_Q.

In this article, we investigate the hadron-quark phase transition of neutron star matter, when the transition proceeds through a mixed phase. The calculation results of the mixed phase structure (Glendenning construction) are compared with the results of a usual first-order phase transition (Maxwell construction). Also, the influence of a δ-meson field on phase transition characteristics is discussed. Finally, using the EOS obtained, we calculate the integral and structural characteristics of neutron stars with quark degrees of freedom.

2 EQUATION OF STATE OF NEUTRON STAR MATTER

2.1 Nuclear Matter

In this section, we consider the EOS of matter in the region of nuclear and supranuclear density ($n \geq 0.1\,\mathrm{fm}^{-3}$). For the lower density region, corresponding to the outer and inner crust of the star, we have used the EOS of Baym-Bethe-Pethick (BBP) (Baym et al. 1971). To describe the hadronic phase we use the relativistic nonlinear Lagrangian density of a many-particle system consisting of nucleons (p, n), electrons and isoscalar-scalar (σ), isoscalar-vector (ω), isovector-scalar (δ), and isovector-vector (ρ) - exchanged mesons [1]

$$
\begin{aligned}
\mathcal{L} =\ & \overline{\psi}_{N}[\gamma^{\mu}(i\partial_{\mu} - g_{\omega}\omega_{\mu}(x) - \frac{1}{2}g_{\rho}\boldsymbol{\tau}_{N}\boldsymbol{\rho}_{\mu}(x)) - (m_{N} - g_{\sigma}\sigma(x) - g_{\delta}\boldsymbol{\tau}_{N}\boldsymbol{\delta}(x))]\psi_{N} \\
& + \frac{1}{2}(\partial_{\mu}\sigma(x)\partial^{\mu}\sigma(x) - m_{\sigma}\sigma(x)^{2}) - U(\sigma(x)) + \frac{1}{2}m_{\omega}^{2}\omega^{\mu}(x)\omega_{\mu}(x) - \frac{1}{4}\Omega_{\mu\nu}(x)\Omega^{\mu\nu}(x) \\
& + \frac{1}{2}(\partial_{\mu}\boldsymbol{\delta}(x)\partial^{\mu}\boldsymbol{\delta}(x) - m_{\delta}^{2}\boldsymbol{\delta}(x)^{2}) + \frac{1}{2}m_{\rho}^{2}\boldsymbol{\rho}^{\mu}(x)\boldsymbol{\rho}_{\mu}(x) - \frac{1}{4}\Re_{\mu\nu}(x)\Re^{\mu\nu}(x) \\
& + \overline{\psi}_{e}(i\gamma^{\mu}\partial_{\mu} - m_{e})\,\psi_{e}\,,
\end{aligned}
\tag{1}
$$

where $x = x_{\mu} = (t, x, y, z)$, $\sigma(x)$, $\omega_{\mu}(x)$, $\boldsymbol{\delta}(x)$, and $\boldsymbol{\rho}^{\mu}(x)$ are the fields of the σ, ω, δ, and ρ exchange mesons, respectively, $U(\sigma)$ is the nonlinear part of the potential of the σ-field, given by Boguta & Bodmer (1977)

$$
U(\sigma) = \frac{b}{3}\,m_{N}(g_{\sigma}\sigma)^{3} + \frac{c}{4}\,(g_{\sigma}\sigma)^{4},
\tag{2}
$$

m_{N}, m_{e}, m_{σ}, m_{ω}, m_{δ} and m_{ρ} are the masses of the free particles, $\psi_{N} = \begin{pmatrix} \psi_{p} \\ \psi_{n} \end{pmatrix}$ is the isospin doublet for nucleonic bispinors, and $\boldsymbol{\tau}$ are the isospin 2×2 Pauli matrices. The bold face type denotes vectors in isotopic spin space. This Lagrangian also includes antisymmetric tensors of the vector fields $\omega_{\mu}(x)$ and $\boldsymbol{\rho}_{\mu}(x)$ given by

$$
\Omega_{\mu\nu}(x) = \partial_{\mu}\omega_{\nu}(x) - \partial_{\nu}\omega_{\mu}(x)\,, \quad \Re_{\mu\nu}(x) = \partial_{\mu}\boldsymbol{\rho}_{\nu}(x) - \partial_{\nu}\boldsymbol{\rho}_{\mu}(x)\,.
\tag{3}
$$

In the RMF theory, the meson fields $\sigma(x)$, $\omega_{\mu}(x)$, $\boldsymbol{\delta}(x)$ and $\boldsymbol{\rho}_{\mu}(x)$ are replaced by the effective mean-fields $\overline{\sigma}$, $\overline{\omega}_{\mu}$, $\overline{\boldsymbol{\delta}}$ and $\overline{\boldsymbol{\rho}}_{\mu}$.

This Lagrangian density (1) contains the meson-nucleon coupling constants, g_{σ}, g_{ω}, g_{ρ} and g_{δ}, as well as parameters of the σ-field self-interacting terms b and c. In our calculations, we take $a_{\delta} = (g_{\delta}/m_{\delta})^{2} = 2.5\,\mathrm{fm}^{2}$ for the δ coupling constant, as given in Refs. Liu et al. (2002); Greco et al. (2003); Alaverdyan (2009a); for the bare nucleon mass $m_{N} = 938.93\,\mathrm{MeV}$, for the nucleon effective mass $m_{N}^{*} = 0.78\,m_{N}$, for the baryon number density at saturation $n_{0} = 0.153\,\mathrm{fm}^{-3}$, for the binding

---

[1] We use the natural system of units with $\hbar = c = 1$.

energy per baryon $f_0 = -16.3\,\text{MeV}$, for the incompressibility modulus $K = 300\,\text{MeV}$, and for the asymmetry energy $E_{\text{sym}}^{(0)} = 32.5\,\text{MeV}$. Five other constants, $a_\sigma = (g_\sigma/m_\sigma)^2$, $a_\omega = (g_\omega/m_\omega)^2$, $a_\rho = (g_\rho/m_\rho)^2$, b and c, can then be numerically determined (Alaverdyan 2009b).

In Table 1 we list the values of the model parameters with and without the isovector-scalar δ meson interaction channel (The models RMF$\sigma\omega\rho\delta$ and RMF$\sigma\omega\rho$, respectively).

Table 1 Model Parameters with and without a δ-Meson Field

	a_σ (fm^2)	a_ω (fm^2)	a_δ (fm^2)	a_ρ (fm^2)	$b\,(10^{-2}\,\text{fm}^{-1})$	$c\,(10^{-2})$
RMF$\sigma\omega\rho\delta$	9.154	4.828	2.5	13.621	1.654	1.319
RMF$\sigma\omega\rho$	9.154	4.828	0	4.794	1.654	1.319

The knowledge of the model parameters makes it possible to solve the set of four equations in a self-consistent way and to determine the re-denoted mean-fields, $\sigma \equiv g_\sigma \bar{\sigma}$, $\omega \equiv g_\omega \bar{\omega}_0$, $\delta \equiv g_\delta \bar{\delta}^{(3)}$, and $\rho \equiv g_\rho \bar{\rho}_0^{(3)}$, depending on baryon number density n and asymmetry parameter $\alpha = (n_n - n_p)/n$. Here $\bar{\delta}^{(3)}$ and $\bar{\rho}_0^{(3)}$ are the third isospin components of corresponding mean-fields. The standard QHD procedure allows us to obtain expressions for energy density $\varepsilon(n, \alpha)$ and pressure $P(n, \alpha)$ of nuclear npe plasma

$$
\varepsilon_{\text{NM}}(n, \alpha, \mu_e) = \frac{1}{\pi^2} \int_0^{k_-(n,\alpha)} \sqrt{k^2 + [m_p^*(\sigma, \delta)]^2}\, k^2 dk + \frac{1}{\pi^2} \int_0^{k_+(n,\alpha)} \sqrt{k^2 + [m_n^*(\sigma, \delta)]^2}\, k^2 dk
$$

$$
+ \frac{b}{3} m_N \sigma^3 + \frac{c}{4} \sigma^4 + \frac{1}{2} \left(\frac{\sigma^2}{a_\sigma} + \frac{\omega^2}{a_\omega} + \frac{\delta^2}{a_\delta} + \frac{\rho^2}{a_\rho} \right) + \frac{1}{\pi^2} \int_0^{\sqrt{\mu_e^2 - m_e^2}} \sqrt{k^2 + m_e^2}\, k^2 dk, \quad (4)
$$

$$
P_{\text{NM}}(n, \alpha, \mu_e) = \frac{1}{\pi^2} \int_0^{k_-(n,\alpha)} \left(\sqrt{[k_-(n, \alpha)]^2 + [m_p^*(\sigma, \delta)]^2} - \sqrt{k^2 + [m_p^*(\sigma, \delta)]^2} \right) k^2 dk
$$

$$
+ \frac{1}{\pi^2} \int_0^{k_+(n,\alpha)} \left(\sqrt{[k_+(n, \alpha)]^2 + [m_n^*(\sigma, \delta)]^2} - \sqrt{k^2 + [m_n^*(\sigma, \delta)]^2} \right) k^2 dk
$$

$$
- \frac{b}{3} m_N \sigma^3 - \frac{c}{4} \sigma^4 + \frac{1}{2} \left(-\frac{\sigma^2}{a_\sigma} + \frac{\omega^2}{a_\omega} - \frac{\delta^2}{a_\delta} + \frac{\rho^2}{a_\rho} \right)
$$

$$
+ \frac{1}{3\pi^2} \mu_e (\mu_e^2 - m_e^2)^{3/2} - \frac{1}{\pi^2} \int_0^{\sqrt{\mu_e^2 - m_e^2}} \sqrt{k^2 + m_e^2}\, k^2 dk, \quad (5)
$$

where μ_e is the chemical potential of electrons,

$$
m_p^*(\sigma, \delta) = m_N - \sigma - \delta, \qquad m_n^*(\sigma, \delta) = m_N - \sigma + \delta \quad (6)
$$

are the effective masses of the proton and neutron, respectively, and

$$
k_\pm(n, \alpha) = \left[\frac{3\pi^2 n}{2} (1 \pm \alpha) \right]^{1/3}. \quad (7)
$$
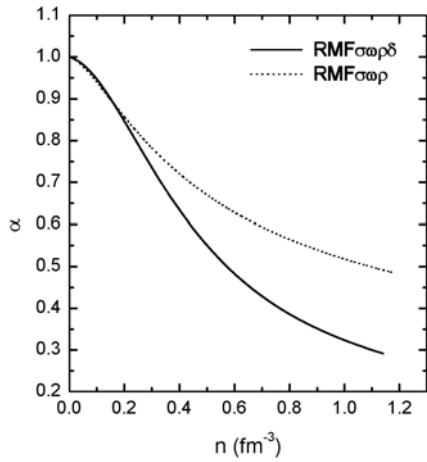
Fig. 1 Asymmetry parameter as a function of the baryon number density n for a β-equilibrium charge-neutral npe -plasma. The solid and dotted lines correspond to the RMF$\sigma\omega\rho\delta$ and RMF$\sigma\omega\rho$ models, respectively.
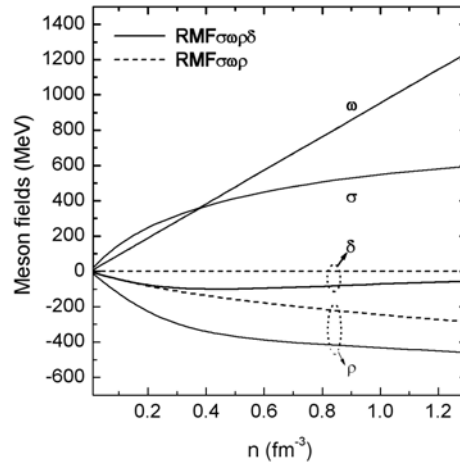
Fig. 2 Re-denoted meson mean-fields as a function of the baryon number density n in case of a β-equilibrium charge-neutral npe-plasma with and without the δ-meson field. The solid and dashed lines correspond to the RMF$\sigma\omega\rho\delta$ and RMF$\sigma\omega\rho$ models, respectively.

The chemical potentials of the proton and neutron are given by

$$\mu_{\mathrm{p}}(n,\alpha) = \sqrt{\left[k_-(n,\alpha)\right]^2 + \left[m_{\mathrm{p}}^*(\sigma,\delta)\right]^2} + \omega + \frac{1}{2}\rho, \tag{8}$$

$$\mu_{\mathrm{n}}(n,\alpha) = \sqrt{\left[k_+(n,\alpha)\right]^2 + \left[m_{\mathrm{n}}^*(\sigma,\delta)\right]^2} + \omega - \frac{1}{2}\rho. \tag{9}$$

In Figure 1, we show the asymmetry parameter α for the β-equilibrium charge-neutral npe-plasma as a function of the baryon number density, n (Alaverdyan 2009a). The solid and dotted lines correspond to the RMF$\sigma\omega\rho\delta$ and RMF$\sigma\omega\rho$ models, respectively. One can see that the asymmetry parameter falls off monotonically with the increase of baryon number density n. For a fixed baryon number density n, the inclusion of the δ-meson effective field reduces the asymmetry parameter α. The presence of a δ-field reduces the neutron density n_{n} and increases the proton density n_{p}.

In Figure 2, we plot the effective mean-fields of exchanged mesons, σ, ω, ρ and δ, as a function of the baryon number density n for the charge-neutral β-equilibrium npe-plasma. The solid and dashed lines correspond to the RMF$\sigma\omega\rho\delta$ and RMF$\sigma\omega\rho$ models, respectively.

From Figures 1 and 2, one can see that the inclusion of the scalar-isovector virtual $\delta(a_0(980))$ meson results in significant changes of species baryon number densities n_{p} and n_{n}, as well as the ρ and δ meson effective fields. This can result in changes of the deconfinement phase transition parameters and, thus, alter the structural characteristics of neutron stars.

The results of our analysis show that the scalar - isovector δ-meson field inclusion leads to the increase of the EOS stiffness of nuclear matter due to the splitting of proton and neutron effective masses, and also to the increase of asymmetry energy (for details see Ref. Alaverdyan 2009a).

2.2 Quark Matter

To describe the quark phase, an improved version of the MIT bag model (Chodos et al. 1974) is used, in which the interactions between u, d and s quarks inside the bag are taken into account in the one-gluon exchange approximation (Farhi & Jaffe 1984). The quark phase consists of three quark flavors, u, d, and s, and electrons, which are in equilibrium with respect to weak interactions. We choose $m_u = 5\,\text{MeV}$, $m_d = 7\,\text{MeV}$ and $m_s = 150\,\text{MeV}$ for quark masses, and $\alpha_s = 0.5$ for the strong interaction constant.

2.3 Deconfinement Phase Transition Parameters

There are two independent conserved charges in the hadron-quark phase transition: baryonic charge and electric charge. The constituent chemical potentials of the npe-plasma in β-equilibrium are expressed through two potentials, $\mu_b^{(\text{NM})}$ and $\mu_{\text{el}}^{(\text{NM})}$, according to conserved charges as follows

$$\mu_{\text{n}} = \mu_b^{(\text{NM})}, \quad \mu_{\text{p}} = \mu_b^{(\text{NM})} - \mu_{\text{el}}^{(\text{NM})}, \quad \mu_{\text{e}} = \mu_{\text{el}}^{(\text{NM})}. \tag{10}$$

In this case, the pressure P_{NM}, energy density ε_{NM} and baryon number density n_{NM} are functions of potentials, $\mu_b^{(\text{NM})}$ and $\mu_{\text{el}}^{(\text{NM})}$.

The particle species' chemical potentials for $udse$-plasma in β-equilibrium are expressed through the chemical potentials $\mu_b^{(\text{QM})}$ and $\mu_{\text{el}}^{(\text{QM})}$ as follows

$$\begin{aligned}
\mu_u &= \frac{1}{3}\left(\mu_b^{(\text{QM})} - 2\,\mu_{\text{el}}^{(\text{QM})}\right), \\
\mu_d &= \mu_s = \frac{1}{3}\left(\mu_b^{(\text{QM})} + \mu_{\text{el}}^{(\text{QM})}\right), \\
\mu_{\text{e}} &= \mu_d - \mu_u = \mu_{\text{el}}^{(\text{QM})}.
\end{aligned} \tag{11}$$

In this case, the thermodynamic characteristics, pressure P_{QM}, energy density ε_{QM} and baryon number density n_{QM} are functions of chemical potentials $\mu_b^{(\text{QM})}$ and $\mu_{\text{el}}^{(\text{QM})}$.

The mechanical and chemical equilibrium conditions (Gibbs conditions) for the mixed phase are

$$\mu_b^{(\text{QM})} = \mu_b^{(\text{NM})} = \mu_b, \qquad \mu_{\text{el}}^{(\text{QM})} = \mu_{\text{el}}^{(\text{NM})} = \mu_{\text{el}}, \tag{12}$$

$$P_{\text{QM}}(\mu_b, \, \mu_{\text{el}}) = P_{\text{NM}}(\mu_b, \, \mu_{\text{el}}). \tag{13}$$

The volume fraction of the quark phase is

$$\chi = V_{\text{QM}} / (V_{\text{QM}} + V_{\text{NM}}), \tag{14}$$

where V_{QM} and V_{NM} are volumes occupied by quark matter and nucleonic matter, respectively.

We applied the global electrical neutrality condition for mixed quark-nucleonic matter, which according to Glendenning is (Glendenning 1992, 2000),

$$\begin{aligned}
&(1 - \chi)\left[n_{\text{p}}(\mu_b, \mu_{\text{el}}) - n_{\text{e}}(\mu_{\text{el}})\right] \\
&+ \chi\left[\frac{2}{3}\,n_u(\mu_b, \mu_{\text{el}}) - \frac{1}{3}\,n_d(\mu_b, \mu_{\text{el}}) - \frac{1}{3}\,n_s(\mu_b, \mu_{\text{el}}) - n_{\text{e}}(\mu_{\text{el}})\right] = 0.
\end{aligned} \tag{15}$$

The baryon number density in the mixed phase is determined as

$$\begin{aligned}
n &= (1 - \chi)\left[n_{\text{p}}(\mu_b, \mu_{\text{el}}) + n_{\text{n}}(\mu_b, \mu_{\text{el}})\right] \\
&+ \frac{1}{3}\,\chi\left[n_u(\mu_b, \mu_{\text{el}}) + n_d(\mu_b, \mu_{\text{el}}) + n_s(\mu_b, \mu_{\text{el}})\right],
\end{aligned} \tag{16}$$

and the energy density is

$$\begin{aligned}
\varepsilon = & (1 - \chi)\left[\varepsilon_{\mathrm{p}}(\mu_b, \mu_{\mathrm{el}}) + \varepsilon_{\mathrm{n}}(\mu_b, \mu_{\mathrm{el}})\right] \\
& + \chi\left[\varepsilon_u(\mu_b, \mu_{\mathrm{el}}) + \varepsilon_d(\mu_b, \mu_{\mathrm{el}}) + \varepsilon_s(\mu_b, \mu_{\mathrm{el}})\right] + \varepsilon_{\mathrm{e}}(\mu_{\mathrm{el}}).
\end{aligned} \tag{17}$$

In the case of $\chi = 0$, the chemical potentials μ_b^{N} and $\mu_{\mathrm{el}}^{\mathrm{N}}$, corresponding to the lower threshold of a mixed phase, are determined by solving Equations (13) and (15). This allows us to find the lower boundary parameters P_{N}, ε_{N} and n_{N}. Similarly, we calculate the upper boundary values of mixed phase parameters, P_{Q}, ε_{Q} and n_{Q}, for $\chi = 1$. The system of Equations (13), (15), (16) and (17) makes it possible to determine the EOS of the mixed phase between these critical states.

Note that in the case of an ordinary first-order phase transition, both nuclear and quark matter are assumed to be separately electrically neutral, and at some pressure P_0, corresponding to the coexistence of the two phases, their baryon chemical potentials are equal, i.e.,

$$\mu_{\mathrm{NM}}\left(P_0\right) = \mu_{\mathrm{QM}}\left(P_0\right). \tag{18}$$

Such a phase transition scenario is known as a phase transition with constant pressure (Maxwell construction).

Table 2 represents the parameter sets of the mixed phase with and without a δ-meson field. It is shown that the presence of the δ-field alters the threshold characteristics of the mixed phase. For $B = 60\,\mathrm{MeV\,fm}^{-3}$, the lower threshold parameters, n_{N}, ε_{N} and P_{N}, are increased; meanwhile the upper ones, n_{Q}, ε_{Q} and P_{Q}, are slowly decreased. For $B = 100\,\mathrm{MeV\,fm}^{-3}$ this behavior changes to the opposite.

Table 2 Mixed Phase Threshold Parameters with and without the δ-Meson Field for Bag Parameter Values $B = 60\,\mathrm{MeV\,fm}^{-3}$ and $B = 100\,\mathrm{MeV\,fm}^{-3}$

Model	n_{N} (fm^{-3})	n_{Q} (fm^{-3})	P_{N} (MeV fm^{-3})	P_{Q} (MeV fm^{-3})	ε_{N} (MeV fm^{-3})	ε_{Q} (MeV fm^{-3})
B60$\sigma\omega\rho\delta$	0.0771	1.083	0.434	327.745	72.793	1280.884
B60$\sigma\omega\rho$	0.0717	1.083	0.336	327.747	67.728	1280.889
B100$\sigma\omega\rho\delta$	0.2409	1.448	16.911	474.368	235.029	1889.336
B100$\sigma\omega\rho$	0.2596	1.436	18.025	471.310	253.814	1870.769

In Figures 3 and 4, we plot the EOS of compact star matter with the deconfinement phase transition for two values of the bag constant, $B = 60\,\mathrm{MeV\,fm}^{-3}$ and $B = 100\,\mathrm{MeV\,fm}^{-3}$, respectively. The dotted lines correspond to pure nucleonic and quark matter without any phase transition, while the solid lines correspond to two alternative phase transition scenarios. Open circles show the boundary points of the mixed phase.

In Figure 5, we plot the particle species number densities as a function of baryon density n for the Glendenning construction. Quarks appear at the critical density $n_{\mathrm{N}} = 0.241\,\mathrm{fm}^{-3}$. The hadronic matter completely disappears at $n_{\mathrm{Q}} = 1.448\,\mathrm{fm}^{-3}$, where the pure quark phase occurs. The solid lines correspond to the case when the δ-meson effective field is also taken into account in addition to the σ, ω, and ρ meson fields (model $B100\_\sigma\omega\rho\delta$). The dashed lines represent the results in the case where we neglect the δ-meson field (model $B100\_\sigma\omega\rho$). One can see that inclusion of the δ-meson field leads to the increase of number densities of quarks and protons, and simultaneously to the reduction of number densities of neutrons and electrons. In Table 2 we have already shown the mixed phase boundaries changes, which are caused by the inclusion of the δ-meson effective field.

Figure 6 shows the constituents' number density as a function of baryon number density n for $B = 100\,\mathrm{MeV\,fm}^{-3}$, when phase transition is described according to the Maxwell construction. The Maxwell construction leads to the appearance of a discontinuity. In this case, the charge neutral
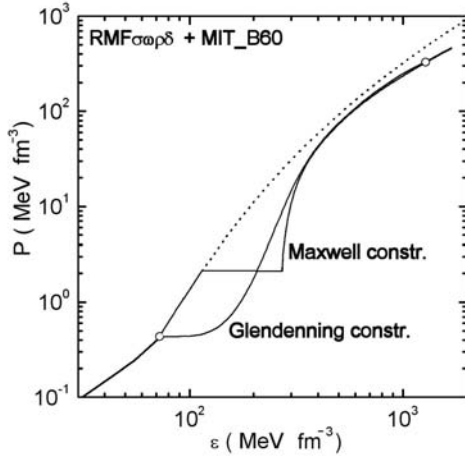
Fig. 3 EOS of neutron star matter with the deconfinement phase transition for a bag constant $B = 60\,\mathrm{MeV}\,\mathrm{fm}^{-3}$. For comparison we plot both the Glendenning and Maxwell constructions. Open circles represent the mixed phase boundaries.
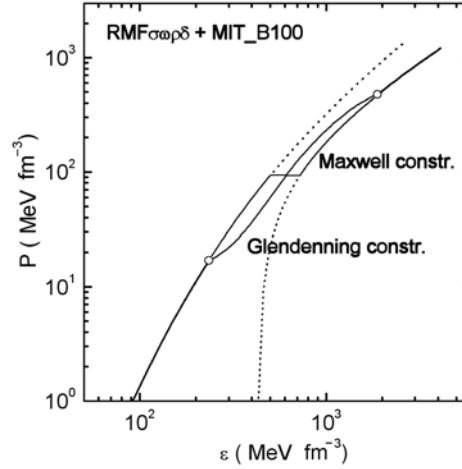
Fig. 4 Same as in Fig. 3, but for B=100 MeV fm^{-3}.
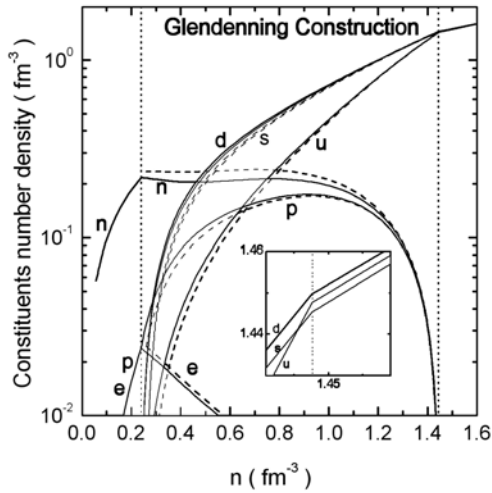
Fig. 5 Constituents' number density versus baryon number density n for B=100 MeV fm^{-3} in the case of the Glendenning construction. Vertical dotted lines represent the mixed phase boundaries. The dashed lines show appropriate results of the model without the δ-meson field.
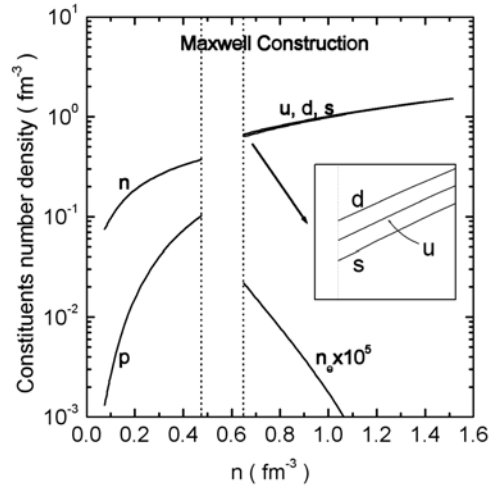
Fig. 6 Same as in Fig. 5, but for the Maxwell construction. Vertical dotted lines represent the density jump boundaries.

nucleonic matter at baryon density $n_1 = 0.475\,\text{fm}^{-3}$ coexists with the charge neutral quark matter at baryon density $n_2 = 0.650\,\text{fm}^{-3}$. Thus, the density range $n_1 < n < n_2$ is forbidden. In case of the Maxwell construction, the chemical potential of electrons, μ_e, has a jump at the coexistence pressure P_0. Notice that such discontinuity behavior takes place only in a usual first-order phase transition, i.e., in the Maxwell construction case.

3 PROPERTIES OF HYBRID STARS

Using the EOS obtained in the previous section, we calculate the integral and structural characteristics of neutron stars with quark degrees of freedom.

The hydrostatic equilibrium properties of spherically symmetric and isotropic compact stars in terms of general relativity are described by the Tolman-Oppenheimer-Volkoff (TOV) equations (Tolman 1939; Oppenheimer & Volkoff 1939)

$$\frac{dP}{dr} = -\frac{G}{r^2}\frac{(P+\varepsilon)(m+4\pi r^3 P)}{1-2G\,m/r}, \tag{19}$$

$$\frac{dm}{dr} = 4\pi r^2 \varepsilon, \tag{20}$$

where G is the gravitational constant, r is the distance from the center of the star, $m(r)$ is the mass inside a sphere of radius r, and $P(r)$ and $\varepsilon(r)$ are the pressure and energy density at the radius r, respectively. To integrate the TOV equations, it is necessary to know the EOS of neutron star matter in a form $\varepsilon(P)$. Using the neutron star matter EOS obtained in the previous section, we have integrated the TOV equations and obtained the gravitational mass M and the radius R of compact stars (with and without quark degrees of freedom) for the different values of central pressure P_c.

Figures 7 and 8 illustrate the $M(R)$ dependence of neutron stars for the two values of bag constant $B = 60\,\text{MeV fm}^{-3}$ and $B = 100\,\text{MeV fm}^{-3}$, respectively. We can see that the behavior of the mass-radius dependence significantly differs for the two types of phase transitions. Figure 7 shows that for $B = 60\,\text{MeV fm}^{-3}$ there are unstable regions where $dM/dP_\text{c} < 0$ between the two stable branches of compact stars, corresponding to configurations with and without quark matter. In this case, there is a nonzero minimum value of the quark phase core radius. Accretion of matter on a critical neutron star configuration will then result in a catastrophic rearrangement of the star, forming a star with a quark matter core. The range of mass values for stars, containing the mixed phase, is $[0.085\,M_\odot; 1.853\,M_\odot]$ for $B = 60\,\text{MeV fm}^{-3}$, and is $[0.997\,M_\odot; 1.780\,M_\odot]$ for $B = 100\,\text{MeV fm}^{-3}$. In the case of a Maxwellian type phase transition, the analogous range is $[0.216\,M_\odot; 1.828\,M_\odot]$ for $B = 60\,\text{MeV fm}^{-3}$. From Figure 8, one can observe that in the case of $B = 100\,\text{MeV fm}^{-3}$ the star configurations with deconfined quark matter are unstable. Thus, the stable neutron star maximum mass is $1.894\,M_\odot$. Our analysis shows that for $B = 100\,\text{MeV fm}^{-3}$, the pressure upper threshold value for the mixed phase is larger than the pressure, corresponding to the maximum mass configuration. Hence in this case, the mixed phase can exist in the center of compact stars, but no pure quark matter can exist. The dash-dotted curve in Figure 8 represents the results in the case when we neglect the δ-meson field (model $B100\_\,\sigma\omega\rho$). One can see that for a fixed gravitational mass, the star with the δ-meson field has a larger radius than the corresponding star without the δ-meson field. The influence of the δ-meson field on the hybrid star properties is demonstrated in Table 3, where we display the hybrid star properties with and without the δ-meson field for minimum and maximum mass configurations. The results show that the minimum mass of hybrid stars and the corresponding radius are increased with the inclusion of the δ-meson field. Notice that the influence of the δ-meson field on the maximum mass configuration properties is insignificant.
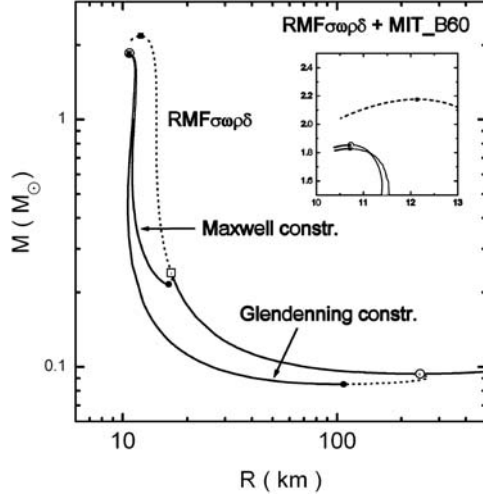
Fig. 7 Mass-radius relation of a neutron star with different deconfinement phase transition scenarios for the bag constant $B = 60\,\mathrm{MeV\,fm^{-3}}$. Open circles and squares denote the critical configurations for the Glendenning and Maxwellian type transitions, respectively. Solid circles and squares denote hybrid stars with minimal and maximal masses, respectively.
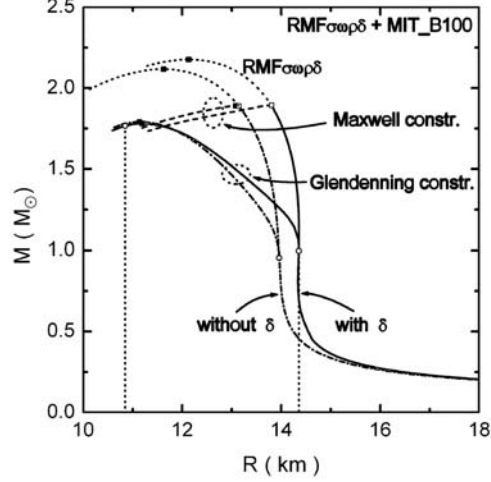
Fig. 8 Same as in Fig. 7, but for $B=100\,\mathrm{MeV\,fm^{-3}}$. The mass-radius relation in the case of the Glendennig construction without the δ-meson effective field is also displayed for comparison (dash-dotted curve).

Table 3 Hybrid Star Critical Configuration Properties for $B = 100\,\mathrm{MeV\,fm^{-3}}$ with and without the δ-Meson Field

Model	Minimum Mass Configuration			Maximum Mass Configuration		
	ε_c (MeV fm^{-3})	$M_{\min}$ ($M_\odot$)	R (km)	ε_c (MeV fm^{-3})	$M_{\max}$ ($M_\odot$)	R (km)
B100$\sigma\omega\rho\delta$	235.029	0.997	14.354	1390.77	1.780	11.190
B100$\sigma\omega\rho$	253.814	0.955	13.960	1386.03	1.791	11.139

4 CONCLUSIONS

In this paper, we have studied the deconfinement phase transition of neutron star matter, when the nuclear matter is described in the RMF theory with the δ-meson effective field. We show that the inclusion of the scalar isovector δ-meson field terms leads to the stiff nuclear matter EOS. In a nucleonic star, both the gravitational mass and corresponding radius of the maximum mass stable configuration increases with the inclusion of the δ field. The presence of the scalar isovector δ-meson field alters the threshold characteristics of the mixed phase. For $B = 60\,\mathrm{MeV\,fm^{-3}}$, the lower threshold parameters, n_N, ε_N, and P_N, are increased, meanwhile the upper ones, n_Q, ε_Q, and P_Q, are slowly decreased. For $B = 100\,\mathrm{MeV\,fm^{-3}}$, this behavior changes to the opposite.

In case of the bag constant value $B = 100\,\mathrm{MeV\,fm^{-3}}$, the pressure upper threshold value for the mixed phase is larger than the pressure, corresponding to the maximum mass configuration. This means that in this case, the stable compact star can possess a mixed phase core, but the density range does not allow it to possess a pure strange quark matter core.

Stars with a δ-meson field have a larger radius than stars of the same gravitational mass without the δ-meson field. Alterations of the maximum mass configuration parameters caused by the inclusion of the δ-meson field are insignificant.

For the bag constant value $B = 60\,\mathrm{MeV\,fm^{-3}}$, the maximum mass configuration has a gravitational mass $M_{\mathrm{max}} = 1.853\,M_{\odot}$ with radius $R = 10.71\,\mathrm{km}$ and central density $\rho_{\mathrm{c}} = 2.322 \times 10^{15}\,\mathrm{g\,cm^{-3}}$. This star has a pure strange quark matter core with radius $r_{\mathrm{Q}} \approx 0.83\,\mathrm{km}$; next it has a nucleon-quark mixed phase layer with a thickness of $r_{\mathrm{MP}} \approx 9.43\,\mathrm{km}$, followed by a normal nuclear matter layer with a thickness of $r_{\mathrm{N}} \approx 0.45\,\mathrm{km}$.

References

Alaverdyan, G. B. 2009a, Astrophysics, 52, 132

Alaverdyan, G. B. 2009b, Gravitation & Cosmology, 15, 5

Baym, G., Bethe, H. A., & Pethick, C. J. 1971, Nucl. Phys. A, 175, 225

Boguta J., & Bodmer, A. R. 1977, Nucl. Phys. A, 292, 413

Chodos, A., Jaffe, R. L., Johnson, K., Thorn, C. B., & Weisskopf, V. F. 1974, Phys. Rev. D, 9, 3471

Farhi, E., & Jaffe, R. L. 1984, Phys. Rev. D, 30, 2379

Glendenning, N. K. 1992, Phys. Rev. D, 46, 1274

Glendenning, N. K. 2000, Compact Stars: nuclear physics, particle physics, and general relativity / Norman
    K. Glendenning (New York: Springer), 2000, (Astronomy and astrophysics library)

Greco, V., Colonna, M., Di Toro, M., & Matera, F. 2003, Phys. Rev. C, 67, 015203

Heiselberg, H., Pethick, C. J., & Staubo, E. F. 1993, Phys. Rev. Lett., 70, 1355

Heiselberg, H., & Hjorth-Jensen, M. 2000, Phys. Rep., 328, 237

Ko, C. M., & Li, G. Q. 1996, Journal of Physics G Nuclear Physics, 22, 1673

Kubis, S., & Kutschera, M. 1997, Phys. Lett. B, 399, 191

Lalazissis, G. A., Konig, J., & Ring, P. 1997, Phys. Rev. C, 55, 540

Liu, B., Greco, V., Baran, V., Colonna, M., & Di Toro, M. 2002, Phys. Rev. C, 65, 045201

Müller, H., & Serot, B. D. 1995, Phys. Rev. C, 52, 2072

Oppenheimer, J., & Volkoff, G. 1939, Phys. Rev. 55, 374

Prassa, V., Ferini, G., Gaitanos, T., Wolter, H. H., Lalazissis, G. A., & Di Toro, M. 2007, Nuclear Physics A,
    789, 311

Serot, B. D., & Walecka, J. D. 1986, in Adv. in Nucl. Phys., eds. J. W. Negele, & E. Vogt, 16

Serot, B. D., & Walecka, J. D. 1997, Int. J. Mod. Phys. E, 6, 515

Tolman, R. 1939, Phys. Rev. 55, 364

Typel, S., & Wolter, H. H. 1999, Nucl. Phys. A 656, 331

Walecka, J. D. 1974, Ann. Phys., 83, 491